

## Hydrodynamic Analysis of a Model Patrol Boat Hull

Balasubramaniam S.\* and Musa M.N.

School of Mechanical Engineering, Faculty of Engineering,  
Universiti Teknologi Malaysia,  
81310 UTM Johor Bahru,  
Johor, Malaysia

\*Corresponding email: sugaanbala@yahoo.com.my

### Article history

Received  
13 November 2019  
Revised  
25 December 2019  
Accepted  
30 December 2019  
Published  
31 December 2019

### ABSTRACT

*This research was conducted with the intent of determining the drag coefficient and study the hydrodynamic behavior around the external body of a model patrol boathull with the aid of Computational Fluid Dynamic (CFD) software using ANSYS CFX version 17.2. The model patrol boat was tested with four variations of speed at 16, 18, 20 and 22 knots in a virtual fluid domain. For the purpose of generating a 3D geometry of the model boat hull, SolidWorks software was used. A turbulent model was selected to simulate the flow field around the external body of the one-meter class sail boat. The final result for this research is the drag coefficient obtained for all variation of speeds. The validation of the results was done by comparing the drag coefficient value from simulation to the established drag coefficient data obtained from the Marine Technology Center (MTC), Universiti Teknologi Malaysia (UTM) on the exact model of a patrol boat used in the simulation.*

**Keywords:** Drag coefficient, computational fluid dynamic, virtual fluid domain

### 1.0 INTRODUCTION

Fluid mechanics is a branch of physics that is concerned with the mechanics of fluids and the forces on them. Advanced fluid dynamics will include the study of turbulence and non-linear flow. These are deemed more exotic areas as they will involve more complex and interesting ideas and mathematics where chaos theory, higher order differential equations, complex algebra and topologies may come into play [1]. If the study involves moving fluids it is usually called *hydrodynamics*. *Hydro* means water, *dynamic* means energy or physical force in motion and effect. Specifically, hydrodynamics refers to the different or ways forces affect the movement of fluids.

The branch of science concerned with the mechanical behavior and properties of fluids in motion is also called hydrodynamics [1]. Hydrodynamics is extensively used many used in many fields such as in boat hull design, propulsion efficiency, pipe flows, flows in pump, channel flows and many more [2]. Hydrodynamics of a boat is the study of the hydrodynamic resistance force on a boat [3]. If an object, such as a boat is immersed in a stream of fluid, the object will be subjected to friction and turbulence. The hydrodynamic study on a boat is very crucial as it gives more understanding on the wide range of complicated phenomena involving fluids.

Understanding these phenomena allow us to make predictions for practical ocean engineering applications such as in boat building [4]. The efficiency of a boat can be analyzed by obtaining its value of drag coefficient value which is denoted as  $C_d$ . The drag coefficient is a dimensionless number which indicates how well a boat can move through water. The lower the value of drag coefficient of the boat, the more efficient the boat is.

Thus, this means it can move more easily through the water. There are several methods that can be used to study the hydrodynamics of a boat and one of these methods is the computer-based simulation method using Computational Fluid Dynamic (CFD).

## 2.0 LITERATURE REVIEW

The study of hydrodynamic of a boat details on how well and stable a boat can move through water. Basically, there are two interacting flow fields of a boat's hydrodynamic. The two interacting flow fields are: the flow past a boat hull and the flow past the boat components such as its propellers, rudder blade and fin. The flow past the boat hull and boat components are categorized as external and unlike a car's aerodynamic, there is no internal fluid flow to be concerned with [5].

In a scenario whereby an object is immersed in a flowing fluid, its frontal region is subjected to a stagnation point. When an object experiences a stagnation point, the velocity of the flowing fluid is low but the pressure subjected onto the object is high. The fluid flow will take the shape of the object. The regions whereby the flow does not take the shape of the object is known as inviscid. In the end region, the flow begins to separate and results in a wake region. The pressure around the end region is low and the fluid molecules tend to cling on to a submerged body which moves through the fluid [6]. This is because the fluid molecules are very close to the surface of the submerged object. Due to the fluid viscosity, these molecules decrease the velocity of the adjacent molecules. At one point, this viscous force will stop affecting the flow. This means the velocity of fluid flow further from the surface will slowly increase. The region between the point that is not affected by viscous effect and surface of object is known as the boundary layer [7]. A model patrol boat hull specification is listed in Table 1.

**Table 1:** Model patrol boat hull specification

	<b>Ship</b>	<b>Model</b>	<b>Unit</b>
	Condition: 1 (Full load)		
Size	20	1	
Draught	1.89	0.0945	m
Length of water line (LWL)	36.1	1.805	m
Wetted surface area	256.52	0.6413	m <sup>2</sup>
Displacement	204.16	25.52	kg
Breadth	7	0.35	m

Drag is the resistance force that acts in the longitudinal axis of the boat, caused by the motion of the boat through water. A drag force is exerted opposite to the direction of the oncoming fluid flow velocity. It is important to remember that the net drag is a combination of pressure drag and friction drag [8]. Figure 1 suggests that at low velocity, only viscous resistance will have a prominent effect on the total resistance while at higher velocity, other resistance components such as air resistance, wave making resistance and wave breaking resistance contribute greatly to the total hull resistance [9].

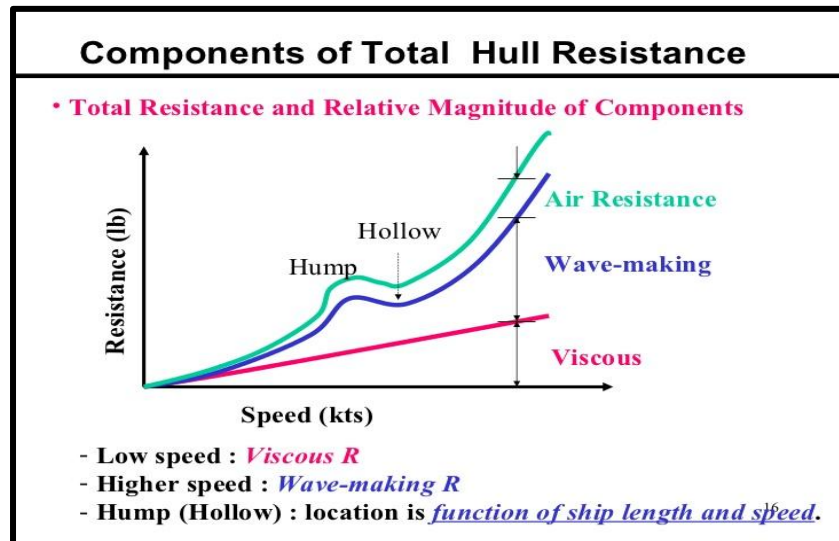


Figure 1: Components of the total hull resistance

CFD has been used by engineers and researchers widely across various fields due to several reasons. CFD uses computational simulation, implying that the costs are relatively inexpensive; the cost of acquiring physical data via experimentations in the laboratory can be drastically reduced. In addition, the CFD simulation can be done within a short period of time and the engineering data can be produced at the early stage of designing. Furthermore, the tool is able to simulate the real condition and has the ability to theoretically stimulate any physical conditions. On top of that, CFD can simulate ideal conditions as the program is capable to isolate specific phenomenon for the study [10].

### 3.0 METHODOLOGY

There are three objectives need to be covered in this research. The first objective is to design a model patrol boat as per the off-set data provided by the MTC. The second objective is to visualize and analyze the fluid flow of the model patrol boat using the *CFX* tools simulation with varying fluid velocities of 16, 18, 20 and 22 knots. Last but not least is to compare the value of the drag coefficient in simulation with the validated result from the MTC.

In order to fulfil this project's requirement, there are a number of steps that need to be taken. The first step is to understand and search for any literature related to the study by acquiring as much information as possible on the research. The next step is to design the hull form geometry of the model patrol boat using the *SolidWorks* software. The dimension for the model patrol boat is provided by the MTC, UTM. After designing the model boat in *SolidWorks*, the model is imported into *ANSYS CFD* to create meshing using its *CFX* tools. The analysis of a boat by numerical simulation was done using the CFD technique. The two softwares used for this part of the project were *SolidWorks* and *Ansys CFX*. *SolidWorks* was used for the construction of the model boat hull, while *Ansys CFX* were used for the simulation part. The overall process flow of the research implementation is illustrated in the flow chart of Figure 2.

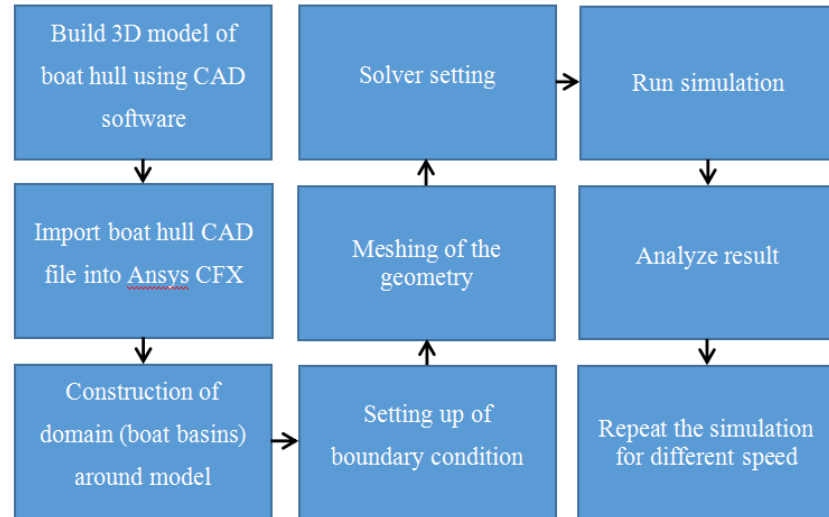


**Figure 2:** Overall process flow for simulation

This boat is designed based on the off-set value and line drawing of a model patrol boat provided by the MTC. The model itself was built using *SolidWorks* using a scale of 1:20 relative to its original specification. There was some simplification made on the model drawing by eliminating or ignoring some features of the boat. This was done to smoothen the result and ease the simulation process. For the results validation, after analyzing the model patrol boat using *CFX* software, the resistances and drag coefficient for the simulation was collected. To make sure the results of the thesis are correct, the results obtained from the simulation was compared to the results provided by MTC. Before comparing the results, the boundary conditions and the dimension of the model need to be exactly the same as those used in the experiment so that the method used in this study is deemed correct, consistent and accurate.

#### 4.0 RESULTS AND DISCUSSION

In this section, the analysis of the CFD simulation results shall be done both quantitatively and qualitatively. The variation of the speed was compared and the hydrodynamic behavior analyzed along with the drag coefficient value. In this simulation, the range of the testing speed was set from 16 to 22 knots with an increment of 2 knots. The final result of the drag coefficient was calculated from the simulation and the average value shall be taken as the research finding. The results as shown in Table 2 were later validated by comparing them with the data provided by the MTC for the same model boat set under similar operating conditions.

**Table 2:** Coefficients of drag corresponding to speed variation from validated experimental results

Speed, $V_s$ (knots)	$V$ (m/s)	$V_m$ (m/s)	$R_{tm}$ (N)	$C_d$
16	8.23	1.84	10.911	0.01028
18	9.03	2.07	12.707	0.009276
20	10.29	2.3	14.779	0.008739
22	11.32	2.53	14.464	0.008046

*Note:*

$R_{tm}$ : Total boat hull resistance,  $V_s$ : Speed relative to the full-scale boat,  $V$ : Speed relative to the full-scale boat,  $V_m$ : Scaled down speed via similarity analysis and  $C_d$ : Drag coefficient.

Utilizing the default setting in ANSYS for mesh generation, a simple default mesh can be generated. A finer mesh is required to produce better results as finer mesh yields more accurate result. Firstly, the mesh sizing parameter can be altered to make a finer mesh using the *relevance center* option. For the sizing of the mesh, the *proximity and curvature* option is chosen as it will make smaller cells around the curves like the leading edges of the hull. Figure 3 shows the mesh generated.

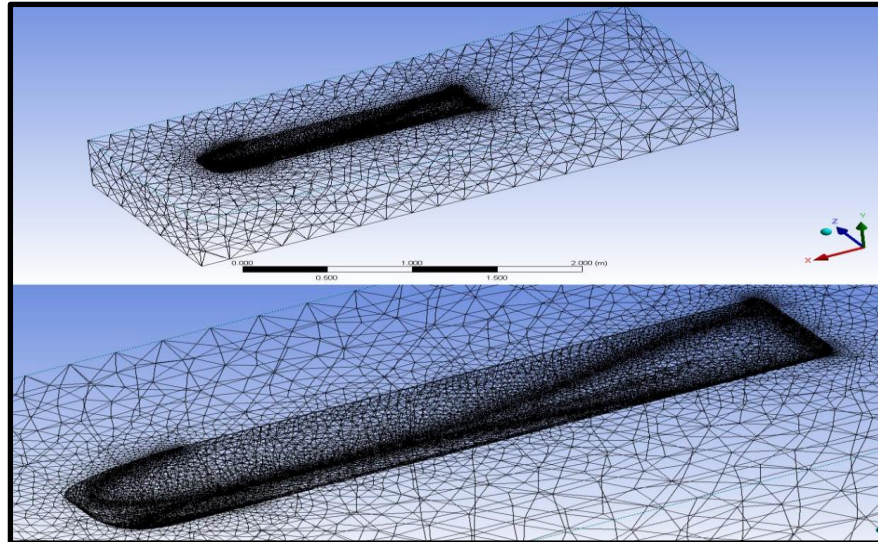


**Figure 3:** Mesh generated via default setting

Due to fluid acceleration, there are gradient of the velocities that can be seen in the boundary layer as shown in Figure 4. In order to get accurate results, the boundary layer using inflation layer needs to be resolved. If the inflation layer is not done, it could lead to incorrect physics that may lead to over or under generate drag, lift, separation, turbulence and resistance.

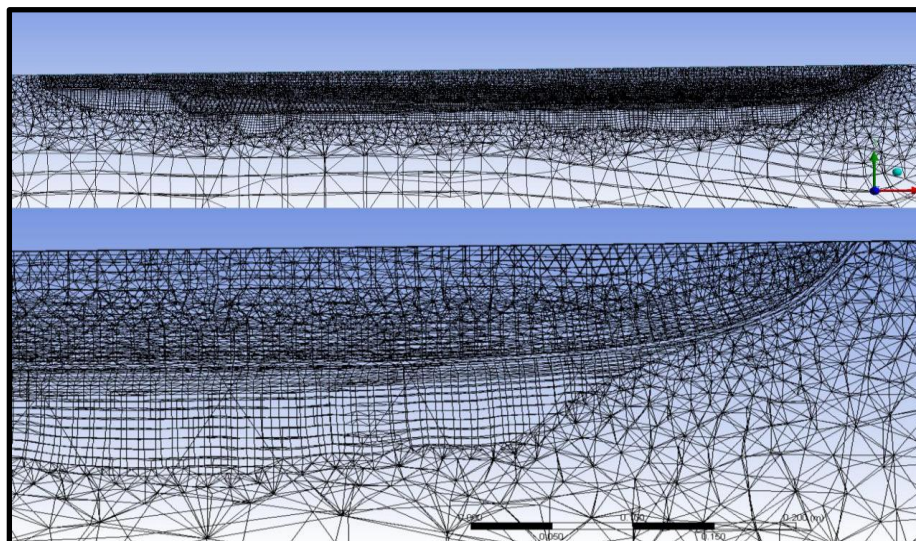


**Figure 4:** Inflation meshing generation cut at Y-section plane

Another technique based on the study in [11] is by building a local refinement box around the hull as shown in Figure 5. This box functions as a limiter where the element

size is restrained to a certain size, typically smaller than the domain itself. The benefit of this control volume is that it makes the overall simulation run faster as a result of reducing the element size. This directly limit the high resolution of mesh in particular areas rather than using high resolution on the entire domain. Figure 6 shows the mesh created with hull refinement box.

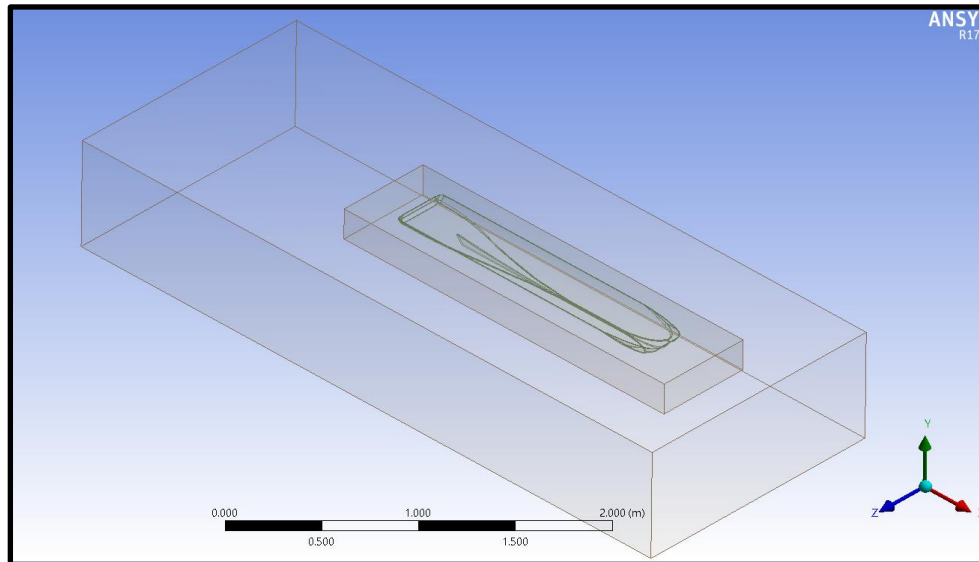


**Figure 5:** Hull refinement box created around the model boat hull

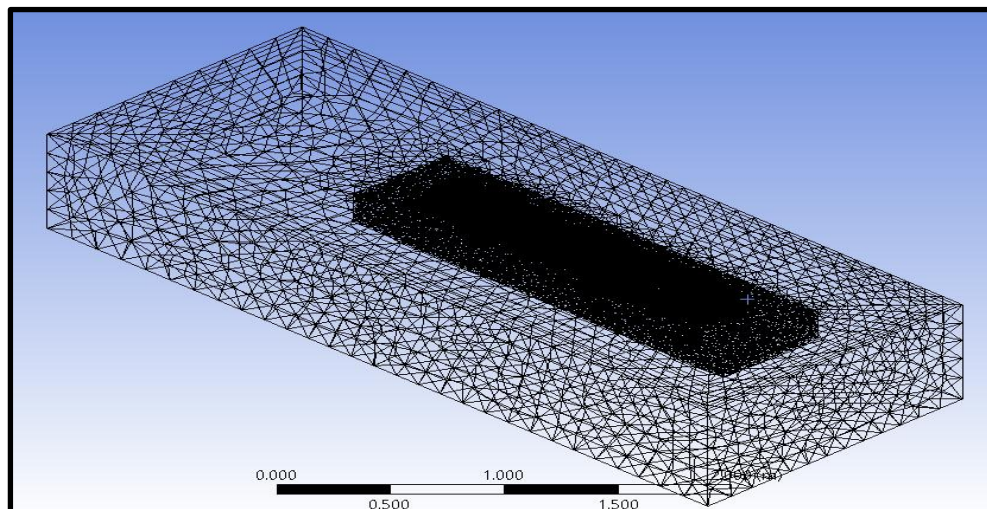


**Figure 6:** Mesh with hull refinement box

A physical domain setting with water medium at a standard temperature condition of  $22.7^{\circ}\text{C}$  was specified and a volume of the fluid model was also selected as it is recommended for free surface flow where the free surface is well defined over the entire domain. For this simulation, the turbulence model was created and used. Each and every surface of the computational domain was named relative to its purpose and role. To ensure the numerical solver recognizes the characters of the boundary condition and apply them automatically, the names given for the boundary conditions follow a set of formats as shown in Figure 7 and Table 3.

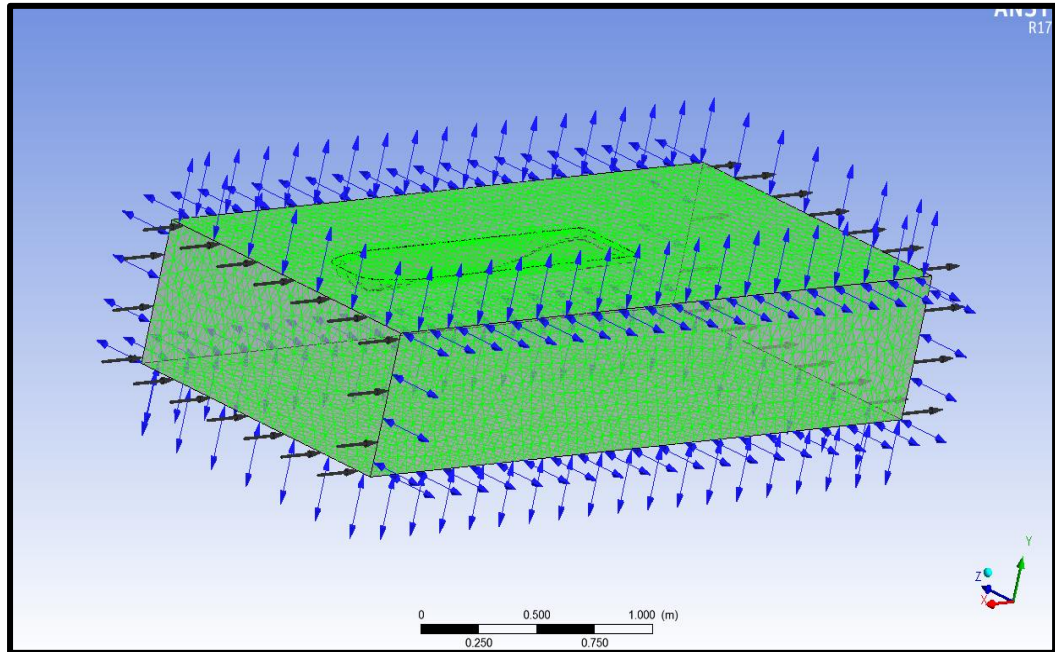


**Figure 7:** Boundary conditions

**Table 3:** Boundary conditions and operational setting

		CASE 1	CASE 2	CASE 3	CASE 4
Velocity inlet	Magnitude	16 knots	18 knots	20 knots	22 knots
	Direction	Positive X direction			
Pressure outlet	Gage pressure magnitude	0 Pa			
	Gage pressure direction	Normal to boundary			
Wall zones	No slip				
Fluid properties	Fluid type	Water			
	Density ( $\text{kg/m}^3$ )	997			
	Viscosity ( $\text{kg/ms}$ )	0.0009396			
Area ( $\text{m}^2$ )	0.661196				

The mesh independence test is conducted prior to the commencement of the real simulation. Using different number of elements, the mesh is tested so that the result of  $Cd$  is independent from the number of elements. Other parameters such as the fluid properties, speed and 3D model are kept constant. For the purpose of this study, the speed for all variation of the number of elements were kept constant at 16 knots.

From Table 4, CASE 1 shows a very coarse mesh size with 122593 elements and a resulting  $Cd$  of 0.01478. This number is very far fetched compared to  $Cd$  of the validated data of just 0.01028. On the other hand, the finest mesh resolution from CASE 6 shows to have 19111108 elements and a resulting  $Cd$  of 0.01098. Referring to Table 4, CASES 1 to 3 only requires few minutes to mesh. This suggests that the meshing for CASES 1 to 3 is quite coarse. The meshing time increased exponentially after the number of elements was increased to 2311996 which indicates a finer mesh was produced. For CASES 5 and 6, the number of elements is generally higher compared to the other cases but the coefficients of drag produced for both cases are very close in value. Thus, to avoid unnecessary waste in time and computational effort, it is wise to stop the mesh at CASE 5.

**Table 4:** Drag coefficient and computed time with respect to the number of elements

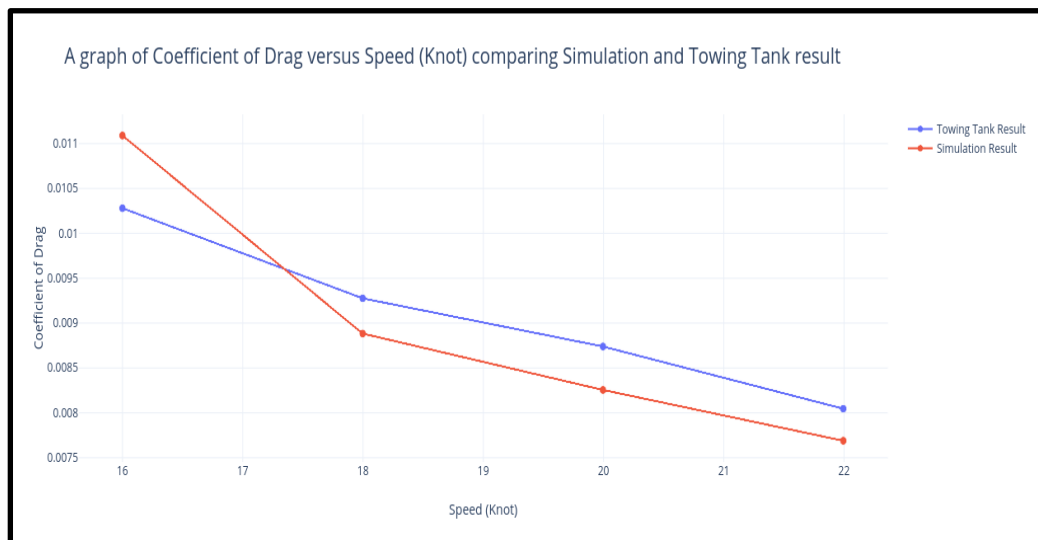
CASE	Element size (m)	Nodes	Element	Time (min)	$C_d$
1	0.06	51082	122593	15	0.01478
2	0.05	84841	205444	23	0.01343
3	0.04	147988	362586	45	0.01139
4	0.03	274606	717341	121	0.01112
5	0.02	773848	2311996	270	0.01109
6	0.01	4843837	19111108	370	0.01098

From the analysis using *ANSYS CFXtools* simulation software, the total resistance force for each model was obtained as shown in Table 5. The variable for the analysis is the speed. The value of the resistance will be converted to dimensionless unit by using the total resistance coefficient formula. Then, the coefficient of the resistance for the model patrol boat will be compared to the experimental data.

**Table 5:** Simulation results

Speed, $V_s$ (knots)	$V$ (m/s)	$V_m$ (m/s)	$R_{tm}$ (N)	$C_d$
16	8.23	1.84	12.384	0.01109
18	9.03	2.07	12.553	0.008883
20	10.29	2.30	14.393	0.008255
22	11.32	2.53	16.221	0.007689

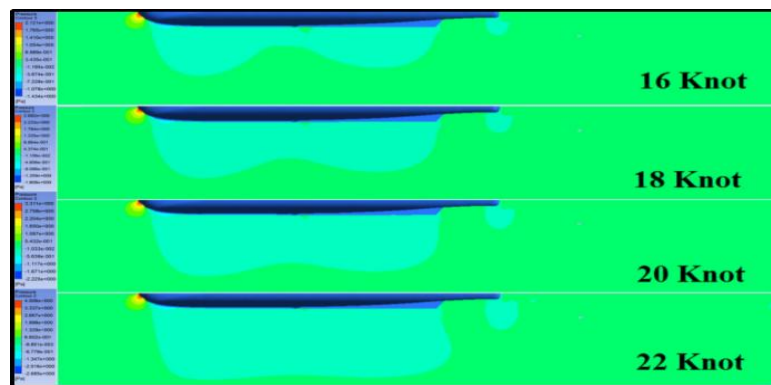
The average  $C_d$  for the experiment and simulation studies are 0.0091 and 0.0087, respectively. The difference between the validated results with the simulation work is only 4.39%. Due to some unexpected error, the value of  $C_d$  for the speed, 16 knots in the simulation ended up higher compared to the validated results from the experiment. From Tables 2 and 5, it can be seen that the drag coefficient from the experimental result is higher compared to the simulation. The hull resistance obtained from the experimental result is higher compared to the simulation counterpart. This may be due to the absence of the air resistance, wave breaking resistance and wave making resistance in the simulation. Figure 8 illustrates the differences between the validated results and the simulation counterpart.



**Figure 8:** Drag coefficient versus speed based on simulation and experimental results

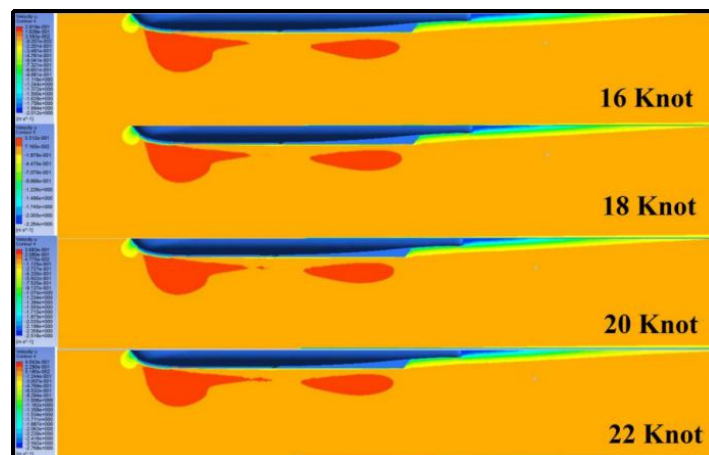


Figure 9 shows the pressure contour for flow field around the boat hull in symmetry plane. It can be observed that high pressure occurs at the frontal part of the boat keel due to the water hitting the boat in the forward direction to the hull. Through observing the cases for all speed variation, it is evident that the positive pressure at the frontal area of the boat is marked by the red region. The negative pressure, on the other hand occurs at the rest of the boat hull as water molecules accelerates across the boat hull. The highest pressure is generated at the frontal area of the boat keel because the fluid flow experiences a stagnation condition. The stagnation condition occurs when the velocity of fluid is zero at the local point in which is subjected to direct contact with the boat keel. This phenomenon complies with *Bernoulli's* equation in which states that the pressure increases as the velocity decreases. For this case, the pressure is at its peak when the velocity is zero.



**Figure9:** Pressure contour distribution for all speed variation

To validate the phenomenon mentioned for the pressure contour as shown in Figure 9, the velocity contour for the field flow around the boat hull in symmetry plane can be observed in Figure 10. At the frontal part of the boat, especially at the keel, the velocity of the fluid flow is relatively low. There also appears to be a very thin layer of low-velocity contour to be formed around the boat hull. This scenario happens due to the fluid flow resistance to viscous surface on the boat hull. It can be seen from Figure 10 that the regions further from the hull produced greater velocity compared to other areas.



**Figure10:** Side view of the velocity distribution contour around the model boat body for all speed variation

Figure 11 shows the water streamline vector flow direction around model patrol boat, signifying the water direction throughout the hull. As can be seen in the figure, when the water flows, it did not produce any turbulence at the midway through the hull; this indicates the shape of the hull moves easily through the water even at low speeds. When the water collides with the frontal keel of the boat hull, the water dissipates around it and in turn produces high velocity waves. If Figure 11 is closely observed, there is a separation of flow occurring on the side of the boat hull for each case. This phenomenon happens as a result of the energy loss of the flow due to the viscous effect on the boat hull surface. Also, it is observed that as the velocity of fluid flow increases, the separation of the flow becomes delayed. In CASE 1 at 16 knots, the separation flow occurs earlier compared to CASE 4 at 22 knots. As a consequence of the separation flow, regions known as eddies were created. These regions are better known as wakes. The cluster of small rotating regions or loops behind the model boat from all the cases can be seen in Figure 11. It represents the eddies and as the velocity of the fluid flow increases, the wake region shrinks. The shrinking of the wake region reduces the drag, especially those related to the pressure drag. As the fluid flow velocity increases, so does the intensity of the streamline re-circulation. As an evidence, it can be seen in Figure 11 that for CASE 1, with fluid velocity at 16 knots, there appears to be a larger wake region. Also, in the figure, a lower re-circulation intensity is shown, represented by the lightest streamline that produces the thinnest eddies among all cases. In contrast, for CASE 4 with a fluid velocity of 22 knots, it yields smaller wake region as indicated by the red circle and shows the thickest eddies in its streamline. This re-circulation helps to push the hull forward, thus as a result the drag coefficient decreases.

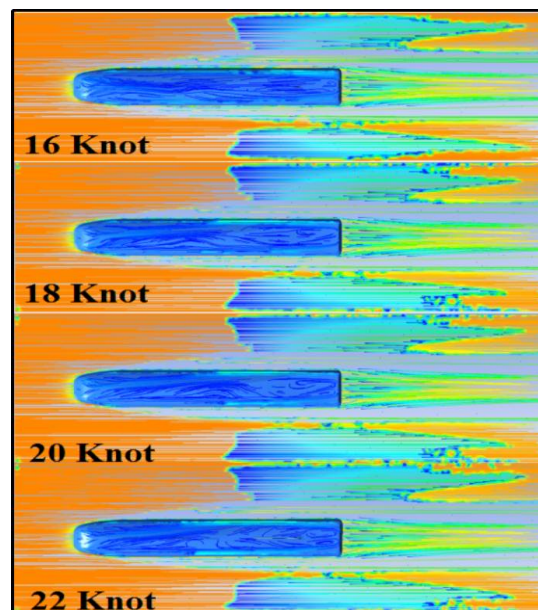


**Figure 11:** Top view of the velocity streamline around the model boat body for all speed variation

## 5.0 CONCLUSION

From the study, it can be concluded that as the delay in the boundary layer separation increases, the wake region forming at the rear end of the model boat is reduced. This reduced wake region will in turn reduce the pressure drag, thus by doing so decreases the drag coefficient of the model boat. From the final simulation results, the average drag coefficient related to the boat model is around 0.009. This value is deemed appropriate and comparable to the validated data from the MTC, differing only about 4.39%. Thus,

the drag coefficient obtained from the study is acceptable and realistic, thereby fulfilling the main objective of the study. It is also proven that the CFD method can produce faster initial results compared to the experimental towing tank method.

## REFERENCES

1. Batchelor G.K., 2000. *An Introduction to Fluid Dynamics*, Cambridge University Press, UK.
2. Rana S., 2012. *Introduction of Hydrodynamics and Its Application*. Retrieved from: [https://www.academia.edu/11743583/Introduction\\_of\\_Hydrodynamics\\_and\\_its\\_Application](https://www.academia.edu/11743583/Introduction_of_Hydrodynamics_and_its_Application). [Accessed: 25 July 2019].
3. *Naval hydrodynamics and hydrodynamic wave ship resistance to the advancement. Ship Hydrodynamics*. Retrieved from: [https://www.mecaflux.com/en/hydrodynamique\\_navale.htm](https://www.mecaflux.com/en/hydrodynamique_navale.htm). [Accessed: 1 August 2019].
4. Techet A.H., 2002. *Hydrodynamics for Ocean Engineering*. Retrieved from: <https://dspace.mit.edu/handle/1721.1/35850?show=full>. [Accessed: 25 July 2019].
5. Techet A.H., 2005. *2.016 Hydrodynamics*, Retrieved from: <https://ocw.mit.edu/courses/mechanical-engineering/2-016-hydrodynamics-13-012-fall-2005/readings/2005reading7.pdf>. [Accessed: 25 July 2019].
6. Scobie J.A., Sangan C.M, Lock G.D., 2014. Flow Visualisation Experiments on Sports Balls, *Procedia Engineering*, 72: 738-743.
7. Epifanov V.M, Klimov A.A. and Trdatyan S.A., 1993. Boundary Layer on a Plate with Directed Injection into the Laminar Stream in Kelleher M.D., Sreenivasan K.R., Shah R.K. and Joshi Y. (Eds), *Experimental Heat Transfer, Fluid Mechanics and Thermodynamics 1993*, Elsevier Science.
8. *Real World Physics Problems*. Retrieved from: <https://www.real-world-physics-problems.com/drag-force.html>. [Accessed: 15 August 2019].
9. Molland A.F., Turnock S.R. and Hudson D.A., 2017. *Ship Resistance and Propulsion with Practical Estimation of Propulsive Power*, 2<sup>nd</sup> Edition, Cambridge University Press.
10. Wortley S., 2013. *CFD Analysis of Container Ship Sinkage, Trim and Resistance*, BEng Mechanical Engineering Project Report, Curtin University.
11. LEAP CFD Team, 2012. *Tips & Tricks: Convergence and Mesh Independence Study*. Retrieved from: <https://www.computationalfluidynamics.com.au/convergence-and-mesh-independent-study/>. [Accessed: 15 August 2019].